minerals

MDPI

Article

Bubble Rise Velocity and Surface Mobility in Aqueous Solutions of Sodium Dodecyl Sulphate and *n*-Propanol

Pavlína Basařová [1,*], Yuliya Kryvel [1] and Jakub Crha [1,2]

[1] Department of Chemical Engineering, University of Chemistry and Technology, Prague, 166 28 Prague, Czech Republic; Yuliya.Kryvel@vscht.cz (Y.K.); jakub.crha@vscht.cz (J.C.)

[2] Institute of Chemical Process Fundamentals of the CAS, 165 02 Prague, Czech Republic

* Correspondence: pavlina.basarova@vscht.cz

Received: 30 October 2019; Accepted: 28 November 2019; Published: 29 November 2019

Abstract: Aqueous solutions of simple alcohols exhibit many anomalies, one of which is a change in the mobility of the bubble surface. This work aimed to determine the effect of the presence of another surface-active agent on bubble rise velocity and bubble surface mobility. The motion of the spherical bubble in an aqueous solution of *n*-propanol and sodium dodecyl sulphate (SDS) was monitored by a high-speed camera. At low alcohol concentrations ($x_P < 0.01$), both the propanol and SDS molecules behaved as surfactants, the surface tension decreased and the bubble surface was immobile. The effect of the SDS diminished with increasing alcohol concentrations. In solutions with a high propanol content ($x_P > 0.1$), the SDS molecules did not adsorb to the phase interface and thus, the surface tension of the solution was not reduced with the addition of SDS. Due to the rapid desorption of propanol molecules from the bottom of the bubble, a surface tension gradient was not formed. The drag coefficient can be calculated using formulas for the mobile surface of a spherical bubble.

Keywords: bubble velocity; bubble surface mobility; surfactant; propanol–water–SDS system

1. Introduction

Alcohols with a short carbon chain (propanol, ethanol and methanol) are used as co-surfactants, co-solvents or solvents in many industrial and pharmaceutical applications and at the same time, are studied due to their atypical physico-chemical properties over a broad range of compositions. They exhibit anomalous behaviour when mixed with water, which was verified to have resulted from the ordered formation of water and alcohol molecules. This is governed by hydration between molecules, hydrophilic interactions and hydrogen bonding [1–5]. At very low concentrations, water molecules surround the molecules of alcohol, which disperse in a monomolecular nature. With increasing concentrations of alcohol, we observe the mixture components' progressive aggregation and finally, at a critical concentration, we can detect clustering. The value of the propanol mole fraction corresponding to this critical concentration lies between 0.07 (determined by the surface tension isotherms [6]) and 0.1 (based on mass spectroscopy and X-ray diffraction [5]). The result is a significant drop in surface tension, significant mixing volume and heat, and a change in bubble surface mobility [7]. Very strong hydrogen bonds also lead to multiple increase in viscosity [6,8,9].

Regarding the mixtures of short-chain alcohols and surfactants, scientific studies usually focus on the surfactant critical micelle concentration and the effect of alcohols on the process of micellization [10–15]. The results of the study [10] show that surface active agents aggregate when alcohol is present in the solution and vice versa, but the mixture of surfactants creates micelles

within the alcohol concentration range in which it is present in bulk in the monomeric form. The concentration at which alcohol molecules begin to create microaggregates depends only moderately on the character and concentration of the present surface active agent and it is close to the concentration obtained for the binary water–alcohol system. In addition, on the basis of surface tension measurements, it was found that the surfactant surface concentration decreases and alcohol surface concentration increases with a rising bulk phase alcohol concentration [16]. Although the effects of the influence of surfactants and alcohol on the liquid–gas interface properties are relatively well documented, no study has yet been reported describing the behaviour of bubbles in these solutions.

Bubble rise due to buoyancy is a highly important fundamental phenomenon that contributes significantly to the hydrodynamics of gas–liquid systems. Many studies have used simple correlations, where the terminal bubble velocity U_b is derived from the forces acting on the bubble in a steady state, primarily buoyancy and drag forces [17,18]. These forces are strongly dependent on the fluid properties (density ρ, dynamic viscosity η) and gravitational acceleration as well as the bubble size and shape. For spherical bubbles rising in stagnant liquids, the terminal velocity is usually given in the form

$$U_b = \sqrt{\frac{4}{3}\frac{(\rho_l - \rho_g)}{\rho_l}\frac{gD_b}{C_D}} \quad (1)$$

where indexes l and g denote a liquid or gaseous phase, g is the gravitational constant, D_b is the bubble diameter, and C_D stands for a drag coefficient that differs in individual correlations. In the case of spherical bubbles, an analogy with the flow of a rigid sphere is used. The development of a symmetric flow pattern around spheres only occurs at a creeping flow, where the bubble Reynolds number Re_b is much less than 1, as seen in Equation (2):

$$Re_b = U_b \rho_l D_b / \eta_l \ll 1. \quad (2)$$

With increasing Re_b, the fore-aft symmetry of the flow is deformed and the wake formation becomes apparent. Here, the inertia of the flow overcomes the viscosity effects. In the case of an "inviscid" spherical bubble rising in pure liquids, the flow does not separate due to the viscosity of the surrounding liquid, which is typically much higher than the viscosity of the gas inside the bubble. As a result, the boundary condition imposed at the bubble surface on the tangential component of the liquid velocity is a zero-shear-stress one rather than a no-slip one [17]. For $Re_b > 50$, the existence of a thin boundary layer and a narrow wake are expected where the vorticity produced by the shear-free condition is confined [17,19]. Within intermediate Reynolds number ranges, $1 < Re_b < 50$, neither the creeping flow nor the liquid with negligible viscosity provide a good starting point for the flow field characterization and thus, no theoretical expression of the drag exists [17]. Therefore, the approximate expressions for the drag coefficient are used. In the case of spherical bubbles, models of Moore [20,21] and Mei [22] are often recommended (Equations (3) and (4)).

$$C_{D,Mei} = \frac{16}{Re_b}\left(1 + \left(\frac{8}{Re_b} + \frac{1}{2}\left(1 + 3.315 {Re_b}^{-1/2}\right)\right)^{-1}\right) \quad (3)$$

$$C_{D,Moore} = \frac{48}{Re_b}\left(1 - \frac{2.21}{{Re_b}^{0.5}}\right) \quad (4)$$

The Moore equation can be used for $Re_b > 50$. If contaminants or surface-active molecules are added to the solution, they begin to adsorb on the phase interface and accumulate in the rear area of the rising bubble. The liquid flow around rising bubbles affects the transport of surfactant molecules, which leads to the unequal distribution of adsorbing surfactant molecules along the bubble surface [23]. The gradients of surface tension along the bubble surface are generated and consequently, Marangoni stresses reducing part of the bubble interface mobility are formed. The drag coefficient increases and the bubble velocity decreases. When the concentration of surface-active agents is

sufficiently high, the reduction of bubble rise velocity is so significant that the drag coefficient corresponds to that of solid particles with a condition of no-slip boundary at the interface. For the drag of solid spherical particles, Schiller and Nauman [24] suggested Equation (5):

$$C_{D,SN} = \frac{24}{Re_b}\left(1 + 0.15{Re_b}^{0.687}\right), \quad (5)$$

and this dependence is also able to be applied to bubbles with surfaces whose surfactants have immobilized [25]. Turton and Levenspiel [26] proposed a comparable relation for bubbles with surfaces that are fully immobilized (Equation (6)):

$$C_{D,TL} = \frac{24}{Re_b}\left(1 + 0.173{Re_b}^{0.657}\right) + \frac{0.413}{1+163000{Re_b}^{-1.09}}\ . \quad (6)$$

There is validity to this relation for $Re_b < 130$. For $Re_b > 130$, $C_{D,TL}$ is equal to 0.95 and is considered constant.

In the case of aqueous solutions of alcohols, it was found that the drag coefficient varied in relation to alcohol concentrations [7]. Alcohol molecules present in solutions with very low propanol concentrations ($x_P \leq 0.005$) diffuse onto the phase interface relatively fast and the solutions behave as surfactant solutions. The bubble drag coefficient increases until the bubble surface is totally immobilized. In a region with an intermediate concentration, the behaviour of the alcohol–water solution changes with an increasing propanol concentration. The molecular bonds between propanol and water are shortened and the surface excess of propanol increases. Chodzinska [6] determined the alcohol activity maxima for propanol at molar concentration $x_P \approx 0.02$. When this maximum is reached, the concentration gradients reduce in relation to the surface tension gradients. The shear stress that the liquid exerts on the bubble surface can be reduced, allowing the gradient of the surface tension to be equalized. As a result, there is facilitation of alcohol molecules desorbing from the phase interface, consequently reducing the drag force [7]. Transitioning to the subsequent region is significant and relates to micro-aggregate formation. The mole fraction value relative to propanol molecule aggregation determined using the surface tension isotherm equals 0.07 [6,7]. In the region with a high propanol concentration ($x_P > 0.07$), all alcohol molecules are located in a cluster network. The alcohol molecule concentration within the bulk liquid exceeds the level neccessary for the surface tension gradient to form. The rate of adsorption of alcohol molecules onto the phase interface is equal to the desorption rate, therefore no molecule accumulation at the bottom of the bubble occurs and no stagnant cap is formed. The liquid flow thus exerts very low shear stress on the bubble surface, which appears fully mobilised [7]. The aim of this study was to evaluate the effect of surfactants on bubble velocity and surface mobility in an aqueous solution of *n*-propanol. Sodium dodecyl sulphate (SDS) has been selected as one of the best known and most widely used surfactants.

2. Materials and Methods

The water purification system "ULTRAPURE", manufactured by Millipore, was used to produce deionised and demineralised water at laboratory temperature for every measurement. Penta supplied > 99.5% pure *N*-propanol, which was used as delivered without further purification. Sigma-Aldrich Chemical Company supplied the sodium dodecyl sulphate with ≥99% declared purity, which adhered to the designated level for ion pair chromatography (catalogue number 71,726) and was used as delivered. A Mettler Toledo NewClassic ML balance with ±0.01g accuracy was used to weigh out appropriate amounts of *n*-propanol and water in preparation for the solutions of aqueous alcohol. For the very dilute solutions, a Mettler Toledo AE 200 balance with ±0.0005 g accuracy was used. So as to ensure a well-distributed mixture, the solution underwent short uniform stirring and was then left at laboratory temperature. The surfactant was added to the mixture after 24 h. Table 1 lists the molar and weight fractions used to express the propanol–water mixture concentrations, along with their related physical properties, namely surface tension, density and viscosity.

A Krűss Bubble Pressure Tensiometer (BP100) (KRÜSS GmbH, Hamburg, Germany) was used to measure the dynamic surface tension in accordance with the maximum bubble pressure method. The bubble age ranged between 10 ms and 1 s.

The freely rising bubble method was used to perform the measurements in glass cells. The details are given in [7]. A bubble generator was used to create individual bubbles, which rose through stagnant liquid. Bubble production occurred at the top of a thin capillary with a 375 μm outer diameter and a 10 μm inner diameter. The bubble rising at terminal velocity was captured on monochrome images at 2000 fps frame velocity using a high-speed 1024H × 1024V pixel Photron SA1.1 camera with a Navitar macro-objective lens and 2–3 px/μm image resolution. From a point of 20 cm from the capillary tip, the camera was set to capture bubble movements. At this distance, no bubble shape acceleration or oscillations were detected. For each of the solutions prepared, between 20 and 30 sequences of bubbles were captured by the camera.

NIS-Elements software was used to analyse and evaluate the captured images. Bubble parameters such as the vertical and horizontal bubble centre positions, bubble circularity and bubble diameter D_b were measured for each frame of all sequences. For each of the sequences, the average bubble diameters were determined using the data obtained. By executing two consecutive shots and determining both bubble centres' x- and y-coordinates, bubble travel distances were calculated. The distance divided by the time it took for that distance to be travelled was used to calculate terminal rising bubble velocities. Minimums of 20 consecutive bubble positions were used to determine average values.

Table 1. The water–propanol solutions and their properties. Molar and mass fractions, experimental density, surface tension and dynamic viscosity at 24 °C.

Molar Fraction x_i	Mass Fraction w_i	Temperature (°C)	Density (kg/m³)	Surface Tension (mN/m)	Dynamic Viscosity (mPa·s)
0	0	24.0	997.3	72.1	0.911
0.001	0.0033	24.0	997.0	68.2	0.923
0.01	0.0326	24.0	992.6	50.4	1.045
0.10	0.2709	24.0	953.8	26.2	2.199
0.30	0.5890	24.0	887.5	25.4	2.810

3. Results and Discussion

3.1. Surface Tension

The surface tension of pure liquids is not dependent on the bubble surface age and the same value should be obtained regardless of the measurement method. For pure water and *n*-propanol, the surface tensions were determined as 72.2 and 23.3 mN/m at 24 °C, respectively. In the case of aqueous alcohol solutions, the dynamic surface tension also does not change over time [7,27]. This is due to the fact that the alcohol and water molecules form a structured network in the surface layer and the concentration of alcohol in the surface layer is higher than in the bulk liquid [6,28]. If there are any changes in local concentration, these changes are very fast (in the order of picoseconds [29]), and cannot be detected by the maximum bubble pressure method. In an aqueous solution of a common surfactant, the surface tension changes over time. A freshly formed interface of a surfactant solution has a surface tension which is very close to that of the solvent. Depending on the concentration and type of surfactant, there is a decay in surface tension until an equilibrium value is reached. This decay occurs over a time period ranging from days to milliseconds. When two surfactants are present in the solution, they interact and frequently exhibit characteristic properties which are remarkably different and have a superior performance from those of individual components. The surface tension decreases relative to the values for the individual surfactants [30].

Figure 1 illustrates the dependence of dynamic surface tension γ_{LG} for aqueous solutions of SDS and propanol as a function of the bubble surface age which represents the time needed to create a new bubble. The equilibrium data are given in Table 2. The data for the aqueous SDS solutions were

taken from [31,32]. At low propanol concentrations, the propanol–SDS mixture behaved as a mixture of surfactants. The surface tension of the aqueous solution of propanol at a concentration of x_P = 0.001 was 68.2 mN/m while the surface tension of the aqueous solution of SDS at a concentration of 0.5 mmol/l was 70.1 mN/m. The aqueous solution of both substances has a surface tension of 63.9 mN/m. Similarly, the surface tension of an aqueous solution of propanol having a concentration of x_P = 0.01 was 50.4 mN/m. The aqueous solution of both substances (x_P = 0.01 and c_{SDS} = 0.5 mmol/L) had a surface tension of 48.9 mN/m. Obviously, both types of molecules were absorbed on the phase interface and a synergistic effect occured. This is consistent with the results published by Janczuk [16], who measured the surface tension of the SDS and propanol solutions (x_P < 0.05). According to this study, the surface adsorption behaviour of the SDS and propanol mixtures at a SDS concentration lower than the critical micelle concentration (CMC, 9.7 mmol/L [31]) can be predicted by using a simple adsorption isotherm.

Table 2. Surface tension of water–propanol–sodium dodecyl sulphate (SDS) solutions.

x_P (Propanol Molar Fraction)	0	0.001	0.01	0.1	0.3
SDS Concentration (mmol/L)	surface tension (mN/m) at 24 °C				
0.5	70.1 [32]	63.9	48.9	26.6	24.9
5	49.3 [32] 46.9 [31]	-	-	26.5	25.3
15	39.0 [32] 39.2 [31]	-	-	26.5	24.6

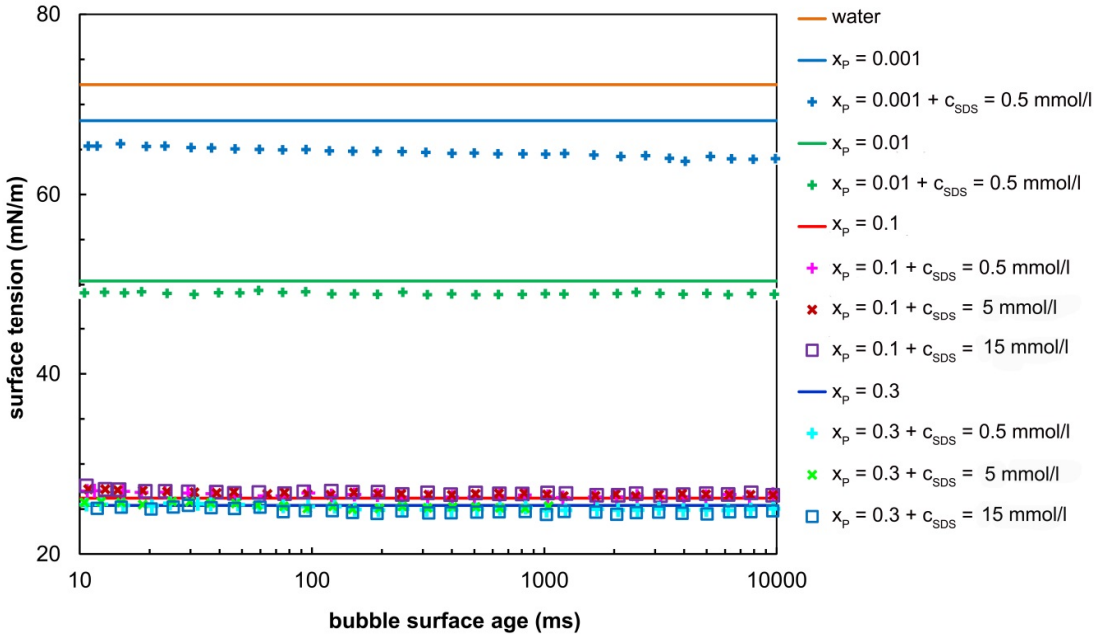

Figure 1. Dynamic surface tension plotted as a function of bubble surface age. The full lines represent the surface tension of water and propanol–water solutions; the symbols represent the data for the water–propanol–SDS mixture. Note: The values of surface tension for concentrated solutions (x_P = 0.1 and x_P = 0.3) overlap.

The effect of SDS diminishes with increasing alcohol concentration. This phenomenon has not been clearly explained. One assumption is that the influence of the propanol on the adsorption behaviour of SDS is stronger than the SDS on propanol adsorption [33], thus the decrease in the surface activity of SDS in water–alcohol solutions could be explained by the competitive adsorption of SDS to alcohols [34]. According to the detailed study made by Bielawska [11], the surface tension values of the aqueous solutions of SDS with propanol above the alcohol CAC (critical aggregation

concentration, x_P = 0.068–0.074,) are nearly the same as those of aqueous solutions of propanol at the same propanol concentration. This assumption indicates that alcohol affects the value of the solution surface tension more than the surfactant. Manko [35] confirmed that the adsorption rate of surfactants is very small or practically zero at the concentration of propanol higher than its critical concentration. According to our measurements (see Table 2 and Figure 1) the surface tension values of the multicomponent mixture with $x_P \geq 0.1$ are almost the same as for the aqueous solutions of propanol at a proper concentration.

3.2. Terminal Bubble Rise Velocity

The data from all of the measurements are given below in Figure 2 where the lines represent the theoretical values that are calculated by Equation (1) and the circles depict the experimental data. The solid line (top) indicates the rise velocity for mobile bubbles where the drag coefficients C_D were calculated by the Mei relation using Equation (3). For bubbles that have immobilized surfaces, the terminal rise velocity is predicted by the dashed line at the bottom with Equation (6) predicting C_D. The calculations used the values listed in Table 1, which shows density values, and Table 2, which shows dynamic viscosity. The data and discussion on bubble velocities in pure water and in aqueous propanol solutions can be found in the literature [7,36].

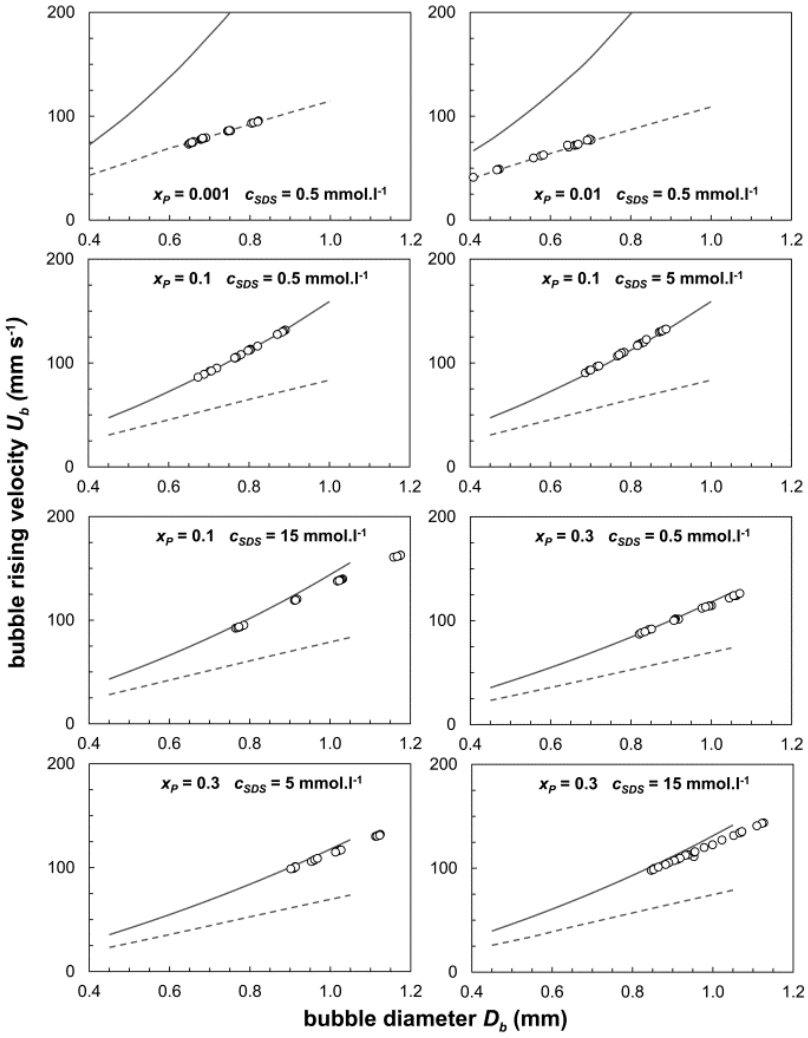

Figure 2. The bubble terminal velocity as a function of bubble diameter in water–propanol–SDS mixtures. The full line represents the calculated velocity for mobile bubble surface. The dashed line represents the calculated velocity for immobile bubble surface.

Bubble size ranges from 0.5 to 1 mm. In solutions with a propanol concentration above 10%, the smallest bubble size is 0.8 mm. This value is given by the capillary diameter and the low surface tension of the solution. In solutions with a low concentration of propanol, the terminal velocity of the bubble is the same as that calculated for bubbles with immobile surfaces. In solutions where x_P is greater than 0.1, the bubble velocity agrees with the velocity calculated for bubbles with a mobile surface. The velocity reduction of bubbles with a diameter above 1 mm is due to the flattening of the bubble. The theoretical velocities were calculated for spherical bubbles, therefore, the deviation of the experimental data from the theoretical values increases. From the graph above, it can be seen that the addition of SDS does not significantly affect the bubble terminal velocity.

3.3. Drag Coefficients and Bubble Surface Mobility

The dependence of the drag coefficient C_D on the bubble Reynolds number Re_b is given in Figure 3. Here, all experimental data are shown. In this figure, the dashed upper line illustrates the drag coefficient for a given Re_b for an immobile bubble surface predicted by Equation (6). The solid lower line gives the drag coefficient for a fully mobile bubble surface for a given Re_b predicted by Equation (3). Clearly, all the experimental data fall in a range that is projected for the immobile and mobile surfaces of bubbles.

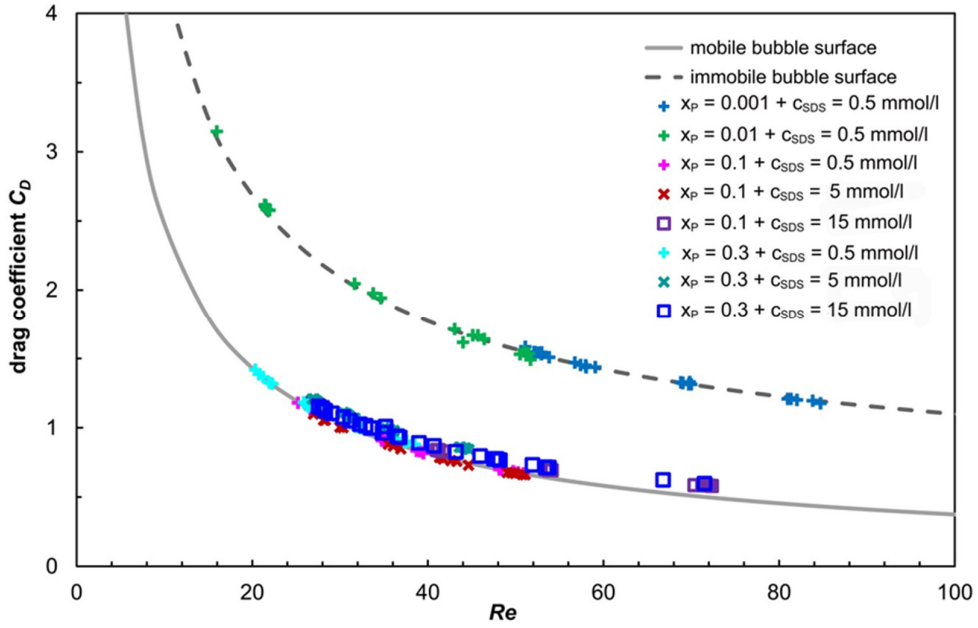

Figure 3. Dependence of the drag coefficient on the bubble Reynolds' number. Dashed line—C_D predicted by Equation (6) (immobile bubble surface). Solid line—C_D predicted by Equation (3) (fully mobile bubble surface).

In aqueous solutions of SDS with a low concentration of propanol (x_P = 0.001 and x_P = 0.01), the drag coefficient is high and can be estimated by the relations for spherical bubbles with immobile surfaces. We can recommend the relationships of Turton and Levenspiel [26] or Schiller and Nauman [24], Equations (5) and (6), respectively. It can be assumed that further increasing of the concentration of SDS will not affect the C_D value. The propanol–SDS mixture behaves as a mixture of surfactants with a synergistic effect. Both types of surface-active molecule adsorb at the phase interface. The smaller propanol molecules are distributed between the larger SDS molecules and form a mixed monolayer on the interface. This effect reduces the surface tension [16,37]. The amount of surfactant adsorbed also defines the boundary between the clean and contaminated interface of the bubble, and can be described using the stagnant cap model [38,39]. For concentrated surfactant solutions, the drag coefficient corresponds to the drag coefficient of solid particles with a no-slip

boundary condition at the interface. Therefore, it can be assumed that a mixture of surfactants with a synergistic effect will form an immobile "cap", even at lower concentrations than the individual solutions of the surfactants themselves. In simple terms, the presence of propanol molecules enhances the immobilization of the bubble surface by SDS molecules.

As the concentration of propanol increases, the synergistic effect disappears. The surface tension values of the multicomponent mixture with $x_P \geq 0.1$ are almost the same as for the aqueous solutions of propanol at a proper concentration. The SDS molecules probably do not adsorb on the interface [35]. In water, the value of the mole fraction corresponding to the molecular aggregation of propanol is equal to 0.07 and all propanol molecules are located in clusters above this concentration [1,6,7]. The surface tension gradient on the phase interface is not formed due to the high concentration of propanol molecules in the bulk liquid. The rate of adsorption and desorption of the alcohol molecules at the phase interface is equal. Therefore, no propanol accumulation at the bottom of the bubble occurs and no stagnant cap is formed [7]. The addition of a surface active agent, here SDS, does not change the properties of the phase interface. At high alcohol concentrations, the formed clusters are so coherent that they will not allow other surfactant molecules to adsorb onto the phase interface and possibly diffuse at a sufficient rate. Furthermore, in a recent study focusing on the dynamics of liquid films in aqueous solutions of NaCl and ethanol between the hydrophobic mica surfaces and the bubble [40], it was demonstrated that surface-active species began departing from air–liquid interfaces as ethanol concentrations rose, which altered the boundary conditions to full mobile or partially mobile. On the basis of our experiments, it is apparent that the surface tension gradient on the bubble surface was not formed in the SDS–propanol–water mixture. In the case of a negligible surface tension gradient, the propanol molecules are rapidly desorbed from the bottom of the bubble (adsorption and desorption rates do not differ) and therefore, the stagnant cap is not formed. The liquid flow creates very low shear stress on the bubble surface and the bubble surface appears to be fully mobilised. In the case of spherical bubbles, the Mei relationship (Equation (3)) or the Moore relationship (Equation (4)) can be used to calculate the drag coefficient C_D.

4. Conclusions

Aqueous solutions of simple alcohols exhibit large anomalies due to their specific arrangement at the molecular level. Based on the experimental results, it was found that alcohol mixtures with another surfactant exhibit similar anomalies. In aqueous solutions of SDS with a low concentration of propanol ($x_P \leq 0.01$), the mixture behaves as a mixture of surfactants with a synergistic effect. The drag coefficient is high and can be estimated by correlations for spherical bubbles with immobile surfaces. The synergistic effect disappears with an increasing propanol concentration. In solutions with a high propanol content ($x_P \geq 0.1$), the addition of SDS does not reduce the surface tension of the solution, and SDS is probably not adsorbed onto the phase interface. Due to the rapid desorption of propanol molecules from the bottom of the bubble, a surface tension gradient is not formed. The drag coefficient can be calculated using formulas for the mobile surface of a spherical bubble.

Author Contributions: P.B. conceived and designed the experiments; J.C. and Y.K. performed the experiments; J.C. analysed the data; P.B. wrote the paper.

Funding: This research was funded by CZECH SCIENCE FOUNDATION (GACR), grant number 19-09518S.

Conflicts of Interest: The authors declare no conflict of interest.

References

1. Dolenko, T.A.; Burikov, S.A.; Dolenko, S.A.; Efitorov, A.O.; Plastinin, I.V.; Yuzhakov, V.I.; Patsaeva, S.V. Raman Spectroscopy of Water-Ethanol Solutions: The Estimation of Hydrogen Bonding Energy and the Appearance of Clathrate-like Structures in Solutions. *J. Phys. Chem. A* **2015**, *119*, 10806–10815, doi:10.1021/acs.jpca.5b06678.
2. Lam, R.K.; Smith, J.W.; Saykally, R.J. Communication: Hydrogen bonding interactions in water-alcohol mixtures from X-ray absorption spectroscopy. *J. Chem. Phys.* **2016**, *144*, doi:10.1063/1.4951010.

3. Banerjee, S.; Ghosh, R.; Bagchi, B. Structural Transformations, Composition Anomalies and a Dramatic Collapse of Linear Polymer Chains in Dilute Ethanol-Water Mixtures. *J. Phys. Chem. B* **2012**, *116*, 3713–3722, doi:10.1021/jp2085439.
4. Dixit, S.; Crain, J.; Poon, W.C.K.; Finney, J.L.; Soper, A.K. Molecular segregation observed in a concentrated alcohol-water solution. *Nature* **2002**, *416*, 829–832, doi:10.1038/416829a.
5. Takamuku, T.; Maruyama, H.; Watanabe, K.; Yamaguchi, T. Structure of 1-propanol-water mixtures investigated by large-angle X-ray scattering technique. *J. Solut. Chem.* **2004**, *33*, 641–660, doi:10.1023/B:JOSL.0000043631.21673.8b.
6. Chodzińska, A.; Zdziennicka, A.; Jańczuk, B. Volumetric and Surface Properties of Short Chain Alcohols in Aqueous Solution–Air Systems at 293 K. *J. Solut. Chem.* **2012**, *41*, 2226–2245, doi:10.1007/s10953-012-9935-z.
7. Basarova, P.; Pislova, J.; Mills, J.; Orvalho, S. Influence of molecular structure of alcohol-water mixtures on bubble behaviour and bubble surface mobility. *Chem. Eng. Sci.* **2018**, *192*, 74–84, doi:10.1016/j.ces.2018.07.008.
8. Pang, F.M.; Seng, C.E.; Teng, T.T.; Ibrahim, M.H. Densities and viscosities of aqueous solutions of 1-propanol and 2-propanol at temperatures from 293.15 K to 333.15 K. *J. Mol. Liq.* **2007**, *136*, 71–78, doi:10.1016/j.molliq.2007.01.003.
9. Vazquez, G.; Alvarez, E.; Navaza, J.M. Surface-Tension of Alcohol Plus Water from 20-Degrees-C to 50-Degrees-C. *J. Chem. Eng. Data* **1995**, *40*, 611–614, doi:10.1021/Je00019a016.
10. Bielawska, M.; Janczuk, B.; Zdziennicka, A. Volumetric properties of sodium dodecylsulfate and Triton X-100 mixture with short-chain alcohol in aqueous solution. *Coll. Surf. A* **2015**, *480*, 270–278, doi:10.1016/j.colsurfa.2014.12.047.
11. Bielawska, M.; Janczuk, B.; Zdziennicka, A. Influence of short chain alcohols on adsorption of sodium dodecylsulfate and Triton X-100 mixture at solution-air interface. *Colloid Surf. A* **2015**, *464*, 57–64, doi:10.1016/j.colsurfa.2014.10.015.
12. Bhattarai, A.; Chatterjee, S.K.; Deo, T.K.; Niraula, T.P. Effects of Concentration, Temperature, and Solvent Composition on the Partial Molar Volumes of Sodium Lauryl Sulfate in Methanol (1) + Water (2) Mixed Solvent Media. *J. Chem. Eng. Data* **2011**, *56*, 3400–3405, doi:10.1021/je2003622.
13. Huang, J.B.; Mao, M.; Zhu, B.Y. The surface physico-chemical properties of surfactants in ethanol-water mixtures. *Coll. Surf. A* **1999**, *155*, 339–348, doi:10.1016/S0927-7757(99)00003-5.
14. Shirzad, S.; Sadeghi, R. Micellization properties and related thermodynamic parameters of aqueous sodium dodecyl sulfate and sodium dodecyl sulfonate solutions in the presence of 1-propanol. *Fluid Ph. Equilib.* **2014**, *377*, 1–8, doi:10.1016/j.fluid.2014.06.009.
15. Zana, R. Aqueous Surfactant-Alcohol Systems—A Review. *Adv. Coll. Interfac* **1995**, *57*, 1–64, doi:10.1016/0001-8686(95)00235-I.
16. Janczuk, B.; Zdziennicka, A.; Wojcik, W. Adsorption of sodium dodecyl sulphate and propanol mixtures at aqueous solution-air interface. *Coll. Surf. A* **2004**, *244*, 1–7, doi:10.1016/j.colsurfa.2004.05.007.
17. Magnaudet, J.; Eames, I. The motion of high-Reynolds-mumber bubbles in inhomogeneous flows. *Annu. Rev. Fluid Mech.* **2000**, *32*, 659–708, doi:10.1146/annurev.fluid.32.1.659.
18. Kulkarni, A.A.; Joshi, J.B. Bubble formation and bubble rise velocity in gas-liquid systems: A review. *Ind. Eng. Chem. Res.* **2005**, *44*, 5873–5931, doi:10.1021/ie049131p.
19. Moore, D.W. The Rise of a Gas Bubble in a Viscous Liquid. *J. Fluid Mech.* **1959**, *6*, 113–130, doi:10.1017/S0022112059000520.
20. Moore, D.W. Velocity of Rise of Distorted Gas Bubbles in a Liquid of Small Viscosity. *J. Fluid Mech.* **1965**, *23*, 749–766, doi:10.1017/S0022112065001660.
21. Moore, D.W. The Boundary Layer on a Spherical Gas Bubble. *J. Fluid Mech.* **1963**, *16*, 161–176, doi:10.1017/S0022112063000665.
22. Mei, R.W.; Adrian, R.J. Flow Past a Sphere with an Oscillation in the Free-Stream Velocity and Unsteady Drag at Finite Reynolds-Number. *J. Fluid Mech.* **1992**, *237*, 323–341, doi:10.1017/S0022112092003434.
23. Cuenot, B.; Magnaudet, J.; Spennato, B. The effects of slightly soluble surfactants on the flow around a spherical bubble. *J. Fluid Mech.* **1997**, *339*, 25–53, doi:10.1017/S0022112097005053.
24. Schiller, L.; Naumann, A. A drag coefficient correlation. *Z. Ver. Deutsch. Ing.* **1935**, *77*, 318–320.
25. Hubicka, M.; Basarova, P.; Vejrazka, J. Collision of a small rising bubble with a large falling particle. *Int. J. Min. Process.* **2013**, *121*, 21–30, doi:10.1016/j.minpro.2013.02.013.

26. Turton, R.; Levenspiel, O. A Short Note on the Drag Correlation for Spheres. *Powder Technol.* **1986**, *47*, 83–86, doi:10.1016/0032-5910(86)80012-2.
27. Basarova, P.; Vachova, T.; Bartovska, L. Atypical wetting behaviour of alcohol-water mixtures on hydrophobic surfaces. *Colloid Surf. A* **2016**, *489*, 200–206, doi:10.1016/j.colsurfa.2015.10.023.
28. Sung, J.H.; Park, K.; Kim, D. Surfaces of alcohol-water mixtures studied by sum-frequency generation vibrational spectroscopy. *J. Phys. Chem. B* **2005**, *109*, 18507–18514, doi:10.1021/jp051959h.
29. Nagasawa, Y.; Nakagawa, Y.; Nagafuji, A.; Okada, T.; Miyasaka, H. The microscopic viscosity of water-alcohol binary solvents studied by ultrafast spectroscopy utilizing diffusive phenyl ring rotation of malachite green as a probe. *J. Mol. Struct.* **2005**, *735*, 217–223, doi:10.1016/j.molstruc.2004.11.014.
30. Rosen, M.J. *Surfactants and Interfacial Phenomena*; John Wiley & Sons: Hoboken, NJ, USA, 2004, doi:10.1002/0471670561.
31. Basarova, P.; Suchanova, H.; Souskova, K.; Vachova, T. Bubble adhesion on hydrophobic surfaces in solutions of pure and technical grade ionic surfactants. *Colloid Surf. A* **2017**, *522*, 485–493, doi:10.1016/j.colsurfa.2017.03.024.
32. Mysels, K.J. Surface-Tension of Solutions of Pure Sodium Dodecyl-Sulfate. *Langmuir* **1986**, *2*, 423–428, doi:10.1021/la00070a008.
33. Zdziennicka, A.; Janczuk, B.; Wojcik, W. Adsorption of mixtures of sodium dodecyl sulphate and propanol at water-air and polytetrafluoroethylene-water interfaces. *Colloid Surf. A* **2004**, *249*, 73–77, doi:10.1016/j.colsurfa.2004.08.054.
34. Kovtun, A.I.; Khil'ko, S.L.; Zholob, S.A.; Rybachenko, V.I. Effect of lower alcohols on adsorption characteristics of sodium dodecyl sulfate solutions at liquid-gas interfaces. *Colloid J.* **2010**, *72*, 389–395, doi:10.1134/S1061933x10030129.
35. Manko, D.; Zdziennicka, A.; Szymczyk, K.; Janczuk, B. Influence of the propanol on the behaviour of binary mixture of nonionic surfactants at the water-air interface. *J. Mol. Liq.* **2014**, *199*, 196–201, doi:10.1016/j.molliq.2014.09.002.
36. Pawliszak, P.; Ulaganathan, V.; Bradshaw-Hajek, B.H.; Manica, R.; Beattie, D.A.; Krasowska, M. Mobile or Immobile? Rise Velocity of Air Bubbles in High-Purity Water. *J. Phys. Chem. C* **2019**, *123*, 15131–15138, doi:10.1021/acs.jpcc.9b03526.
37. Zhu, B.Y.; Rosen, M.J. Synergism in Binary-Mixtures of Surfactants .4. Effectiveness of Surface-Tension Reduction. *J. Colloid Interf. Sci.* **1984**, *99*, 435–442, doi:10.1016/0021-9797(84)90130-9.
38. Dukhin, S.S.; Kovalchuk, V.I.; Gochev, G.G.; Lotfi, M.; Krzan, M.; Malysa, K.; Miller, R. Dynamics of Rear Stagnant Cap formation at the surface of spherical bubbles rising in surfactant solutions at large Reynolds numbers under conditions of small Marangoni number and slow sorption kinetics. *Adv. Colloid Interfac.* **2015**, *222*, 260–274, doi:10.1016/j.cis.2014.10.002.
39. Basařová, P.; Zawala, J.; Zedníková, M. Interactions between a Small Bubble and a Greater Solid Particle during the Flotation Process. *Miner. Process. Extr. M* **2019**, 1–17, doi:10.1080/08827508.2019.1666123.
40. Zhang, X.R.; Manica, R.; Tang, Y.C.; Liu, Q.X.; Xu, Z.H. Bubbles with tunable mobility of surfaces in ethanol-NaCl aqueous solutions. *J. Colloid Interf. Sci.* **2019**, *556*, 345–351, doi:10.1016/j.jcis.2019.08.045.